Journal of the Brazilian Society of Mechanical Sciences and Engineering (2018) 40:175
https://doi.org/10.1007/s40430-018-1116-6

TECHNICAL PAPER

Additive manufacturing of flexible electrically conductive polymer composites via CNC-assisted fused layer modeling process

Narendra Kumar[1] · Prashant Kumar Jain[1] · Puneet Tandon[1] · Pulak M. Pandey[2]

Received: 8 December 2017 / Accepted: 2 March 2018 / Published online: 15 March 2018

Abstract
The applications of electrically flexible conductive polymer composites are rapidly growing over the time due to their widespread use in fabrication of health monitoring devices, sensors, and flexible displays fabrication, etc. Various techniques have been explored to develop electrically conductive polymer composites. In the recent past, fused deposition modeling (FDM) process has been gained tremendous attention to fabricate electrically conductive parts considering rigid polymers along with conductive filler particles. This allows to avail all advantages and benefits of additive manufacturing in the fabrication of complex electrically conductive parts. However, FDM process faces challenges of filament buckling while fabricating flexible parts. Hence, there is need to develop an economically viable and simplified process to fabricate the flexible electrically conductive polymer composite objects. In the present study, fabrication of flexible electrically conductive polymer composite objects has been attempted by developing a novel CNC assisted fused layer modeling process. The developed process uses the material in pellet form instead of a filament, which eliminates the issues of filament buckling and allows flexible object fabrication. The ethylene vinyl acetate (EVA) and graphite (Gr) particles have been used as the polymer matrix and conductive filler material respectively. Solvent and melt blending techniques have been employed to develop EVA/Gr composites. Three-dimensional flexible electrically conductive objects have been fabricated successfully. The experimental result shows the remarkable improvements in electrical conductivity of EVA polymer by incorporation of graphite particles. The outcome of the presented approach may help to fabricate flexible electrically conductive complex structures for soft robotics and electronics applications.

Keywords Elastomers · Ethylene vinyl acetate · Graphite · Additive manufacturing · Fused deposition modeling · Pellets · Flexible electrically conductive composites · Flexible conductive polymers

1 Introduction

The applications of flexible and electrically conductive polymer composites have increased over the time in various fields such as in health monitoring, displays, pressure sensors, and flexible circuit fabrication, etc. [1, 2]. Over the time, the flexible electrically conductive polymer composites have been developed by adding conductive fillers such as carbon fiber, carbon nanotubes, aluminium, copper, graphite, and graphene in the polymer matrix [3–5]. Researchers have used various material processing methods to prepare the conductive polymer composites, which includes melt processing, magnetic stirring, and template methods [6, 7]. These methods are cost effective when simple objects are required but are not suitable for fabrication of complex objects in a short time.

Technical Editor: Márcio Bacci da Silva.

✉ Narendra Kumar
nyiiitj@gmail.com

Prashant Kumar Jain
pkjain@iiitdmj.ac.in

Puneet Tandon
ptandon@iiitdmj.ac.in

Pulak M. Pandey
pmpandey@mech.iitd.ac.in

[1] CAD/CAM Lab, Mechanical Engineering Discipline, PDPM Indian Institute of Information Technology, Design and Manufacturing Jabalpur, Dumna Airport Road, Jabalpur 482 005, India

[2] Mechanical Engineering Department, Indian Institute of Technology Delhi, Delhi, India

Additive manufacturing (AM) has emerged as an advanced technology, which can fabricate complex three-dimensional parts directly from its geometric model [8]. Various AM processes have been developed during the last two decades and now commercially available. Among them, extrusion-based AM processes have shown potential for economic viable solutions due to their cost effectiveness and simple design. The objects made by these processes have shown their worth in various applications such as aerospace, automobile, biomedical, electronics, defense, and food industries. These processes fall into the category of solid-based AM processes where rigid polymer materials are used to fabricate 3D objects [9]. Filament or pellet form materials can be processed, depending upon the design and structure of the system. A small heating element is generally used as a power source for heating material inside the liquefier head or extruder barrel. Then, the heated material in viscous form is deposited on the build platform in layer-by-layer fashion through a small nozzle. During deposition, all layers are fused together and forms a 3D object [10].

Rigid acrylonitrile butadiene styrene (ABS), nylon, and polylactic acid (PLA) and composites are the most examined materials for these processes [11]. Many researchers have explored the polymer composites for improving mechanical, electrical, and thermal properties. Masood et al. experimentally investigated the thermal properties of the developed composite materials of iron particles in the nylon matrix for fused deposition modeling (FDM) process [12]. Results showed that thermal conductivity of the developed composite was sensitive to the filler amount. Torrado et al. fabricated the polymer composites with various filler materials and examined their effects on the part strength [13]. It was found that the highest ultimate tensile strength of parts was increased when printing was done with 5 wt% T_iO_2-reinforced ABS material. Nikzad et al. have studied the effect of iron/ABS and copper/ABS composites on the part strength and found better results when compared with the virgin ABS material [14]. Boparai et al. investigated the effect of aluminium and aluminium oxide in a nylon 6 polymer matrix for fused deposition modeling process [15]. Remarkable improvements have been observed in thermal and wear properties at the cost of mechanical properties. Wei et al. demonstrated graphene-based composite material for 3D printing and obtained results were correlated with the thermal properties [16]. In another study, Rymansaib et al. made the composites by reinforcing carbon nanofibers (CNFs) and graphite flake microparticles in the polystyrene (HIPS) polymer matrix [17]. Results showed the significant improvement in the electrical conductivity of reinforced composite parts. Gnanasekaran et al. printed the electrical conductive structures using CNT and graphene-based polybutylene terephthalate (PBT) materials [18]. They analyzed the electrical conductivity, printability, and mechanical properties of the developed nanocomposites specimens. PBT/CNT showed the better performance than PBT/graphene-made specimens. Leigh et al. developed the conductive composite material for printing of electronic sensors using FDM process [19]. Polycaprolactone (PCL) and carbon black (CB) were chosen as the polymer matrix and filler, respectively. Kwok et al. explored the suitability of polypropylene (PP) and carbon black (CB) materials for making conductive composite filament [20]. The results showed that composites containing more than 25 wt% CB were suitable for printing of conductive parts.

Aforementioned research investigations indicate that researchers have explored the various filler and polymer materials to make composite parts through extrusion-based AM processes. In most of the investigations, relative rigid polymers were used as the matrix material such as ABS, nylon, PLA, etc. Sometimes, flexible objects with specific properties are desirable over the rigid objects in several end-use applications such as wearable sensors, piezo-resistors, etc. It shows that there is a scope for the development of new materials in which more materials including flexible as well as rigid polymers need to be explored. Therefore, the current study aims to develop a flexible electrically conductive polymer composite material for the use in additive manufacturing.

In the current study, graphite (Gr)-filled ethylene vinyl acetate (EVA) polymer composites have been developed to fill the gap between rigid and flexible composites. To the authors' best knowledge, the flexible conductive graphite filled EVA composites through extrusion-based AM process have not been reported yet. A customized extrusion-based CNC-assisted AM process has been developed for fabricating 3D objects using developed composites. The methodology of the current study is shown in schematic diagram in Fig. 1. Highly flexible nature of EVA and its easy processability make it more preferable over the other elastomers. That is why EVA was chosen in the present study as the polymer matrix. Graphite was selected as the filler material due to its excellent electrical properties.

2 Experimental

2.1 Materials

To develop the flexible electrically conductive composites, an elastomer ethylene vinyl acetate (EVA) has been chosen as polymer matrix, while the conductive graphite has been selected as the filler material. EVA is a copolymer of ethylene and vinyl acetate and the percentage of vinyl acetate varies from 0 to 40%. Pellet form EVA with 19% content of vinyl acetate has been used in the current study.

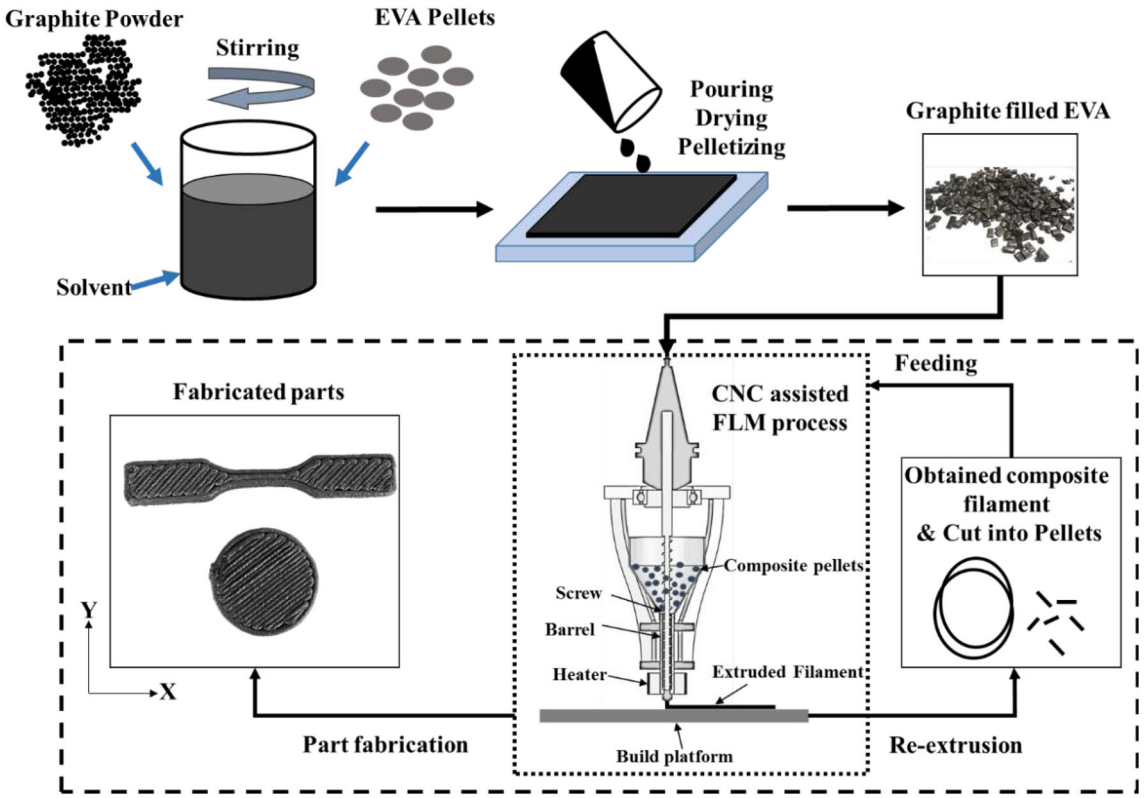

Fig. 1 Schematic representation of proposed work

On the other hand, fine powder of graphite has been used having average particle size of 300 mesh.

2.2 Processing

2.2.1 Preparation of EVA/Graphite composites

The EVA/graphite composite was prepared by taking different wt% of graphite material in EVA polymer matrix as presented in Table 1. The weight percentage of graphite was varied from 20 to 50% in the present study.

The solvent and melt blending processes were utilized to prepare the flexible electrically conductive EVA/Gr composites. These two processes were used for ensuring the homogeneous dispersion of graphite material in EVA matrix. First, the viscous solution of EVA was prepared using the cyclohexane solvent, and then the appropriate amount of graphite was added. The obtained solution was then stirred at 60 °C for 12 h before pouring on a glass plate in the form of a thick sheet. Then, the dried sheet of EVA/Gr composites was kept in the furnace at 82 °C for 1 h for ensuring the solvent removal. After that, the solvent-free composite sheet was cut into small pieces. These pieces were then extruded in the form of a filament. Then, obtained filament was pelletized and extruded again to prepare the test specimens as shown in Fig. 2.

Table 1 EVA and graphite proportions considered in the study

S. no.	EVA (wt%)	Graphite (wt%)
1.	80	20
2.	70	30
3.	60	40
4.	50	50

2.2.2 Newly developed fused layer modeling (FLM) process and parameter setting

An extrusion-based CNC-assisted fused layer modeling (FLM) process has been developed to conduct the study. The developed FLM has different material processing

Fig. 2 Extruded EVA/Gr composite filament and pellets

technique as compared to commercial fused-deposition modeling (FDM) process. Instead of the filament, a developed process using the material in pellet form. Pellet feeding was preferred over the filament because when the flexible filament has processed through commercial FDM, buckling of filament occurs between liquefier head and rollers as shown in Fig. 3.

Due to this reason, printing of flexible parts becomes difficult on commercial FDM. Therefore, in the current study, the material is processed in the form of pellets using developed FLM process. The developed FLM process consists of various key elements, which includes CNC milling machine, screw, barrel, band heater, nozzle, hopper, and supporting frame as shown in Fig. 4. A screw rotates in a counterclockwise direction inside the stationary barrel to process the pellets.

Screw speed and barrel temperature are the critical process parameters for successful printing of specimens on FLM. A 40 W heater is used to melt the EVA/Gr composite. More details about the experimental set up can be found in the literature [21]. To decide the input process parameter settings for EVA material, preliminary experiments were conducted by considering the different levels of process parameters, namely screw speed, barrel temperature, deposition speed. Based on these experiments, it was found that at screw speed 60 rpm, barrel temperature 130 °C, deposition speed 900 mm/min provide good road bonding with controlled dimensions and desired flow rate for EVA. The rheological behavior (melt flow and swelling behavior) of the EVA changed after adding graphite in different proportions. The required value of deposition speed and road width depend on the melt flow rate and swelling behavior of the material being used, for printing. Therefore, based on the obtained results for melt flow and swelling, these two parameters were determined for each composition of EVA/Gr to ensure the proper printing of composite specimens. Other parameters were kept constant as no. of shells at 1, raster angle at ± 45°, road gap at 0 mm and build orientation at *xy*-plane for each material composition. The deposition speed and road width used for printing specimens with each material composition are presented in Table 2.

2.2.3 Preparation of EVA/graphite specimens by FLM

Specimens with different sizes and shapes have been prepared for performing mechanical and electrical tests. For tensile testing, dumbbell-shaped specimens with 3.18 mm width, 25.4 mm clip distance, and 3 mm thickness have been fabricated. A cuboid-shaped specimen has been

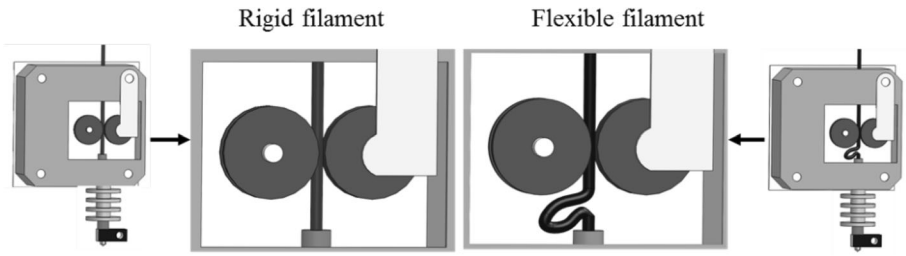

Fig. 3 Buckling occurs with the feeding of the highly flexible filament

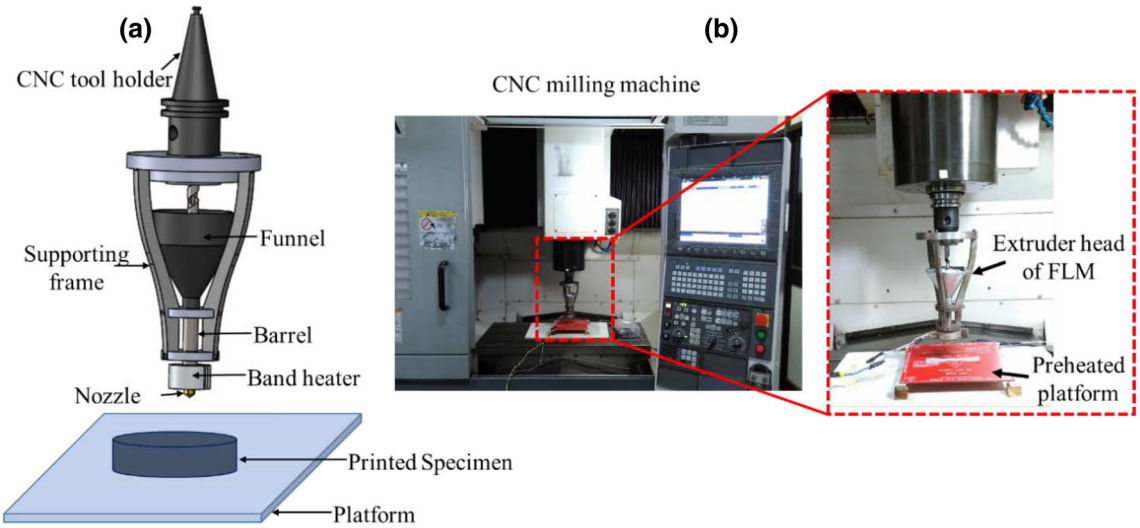

Fig. 4 Developed FLM process. **a** Schematic representation. **b** Actual

Table 2 Used deposition speed and road width for printing specimens with each material composition

S. no.	Parameters	EVA/Gr (wt%/wt)				
		100/0	80/20	70/30	60/40	50/50
1.	Material deposition speed (mm/min)	900	780	500	360	295
2.	Road width (mm)	1.42	1.05	0.95	0.9	0.83

considered for hardness and compression testing with dimensions of 25 mm × 25 mm × 10 mm. Disc shape specimens with 25 mm diameter and 3 mm thickness have been fabricated to determine the electrical properties of the developed composites.

2.3 Material characterization

2.3.1 Morphological analysis of developed composites

Fourier transform infrared spectroscopy (FTIR) analysis is performed to identify the change in the molecular structure using a 'Versatile FTIR Laboratory Spectrometer MB3000'. Pellets of developed composites are used as samples, and FTIR spectra have been collected from the desired regions. All samples have been scanned over 600–4000 cm^{-1} at a resolution of 8 cm^{-1}.

The dispersion and morphology of the developed EVA/Gr composite are studied using scanning electron microscope (SEM). Developed composite pellets have been taken as specimens for SEM observation. All SEM images have been taken using an accelerating voltage of 5 kV.

Further, X-ray diffraction (XRD) has been carried out on a Bruker AXS D8 advance electronic instrument using a step length of 0.020° at 40 kV and 40 mA to see the presence of graphite in the EVA matrix.

2.3.2 Rheology tests

Melt flow rates (MFR) of EVA and EVA/Gr composites was measured by extruding material using melt flow apparatus at 190 °C with a 2.16 kg weight as shown in Fig. 5.

The material was extruded for 10 s. As per ASTM standard, MFR of any material can be measured using the following expression:

$$\mathrm{MFR} = {}^{W}/_{T} \times 600 \quad (1)$$

where *W*/*T* is the weight of extruded material per sec. Thus, a measurement unit of MFR is g/10 min. MFR results have been compared to analyze the change in flow rate of pure EVA and EVA/Gr composites. Further, the developed composites have been extruded through the extruder of FLM before printing specimens to analyze the effect of filler addition on the extruded diameter.

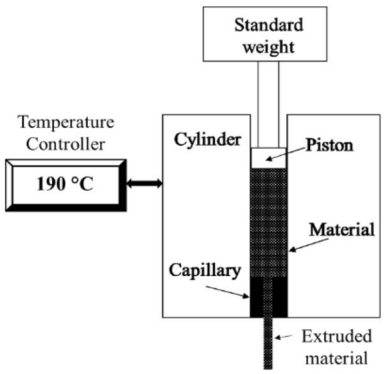

Fig. 5 Schematic diagram of melt flow indexer

2.4 Sample characterization

The electrical conductivity of the developed composite specimens has been determined by a four-probe method (Keithley 2400, Keithley Instruments Inc., USA). The volume resistance of the specimens has been measured first and then converted into the volumetric electrical conductivity using equation.

$$\sigma = \frac{L}{RA} \quad (2)$$

where σ is the electrical conductivity, L is the distance between the two measuring probes (cm), R is the measured resistance (Ω), and A is the effective area of the measuring electrode (cm^2). Disc-shaped specimens have been printed with a diameter of 25 mm and thickness of 2 mm.

The mechanical properties such as tensile strength, elongation, and hardness of the FLM-processed EVA/Gr composites have been evaluated using a universal tensile testing machine (Tinius Olsen). Tests have been performed at a cross-speed of 20 mm/min as per the ASTM-638 standard. The dumbbell-shaped specimens with 3.18 mm width, 25.4 mm clip distance and 3 mm thickness, have been elongated until fracture. Three test specimens have been examined for each developed composite. On the other hand, hardness (shore D) of the developed composite specimens have been measured using a digital durometer. The indenter of the durometer has penetrated into the specimens, and the corresponding values of hardness are recorded.

3 Results and discussion

3.1 Characterization of EVA/graphite composite material

The quality of electrically conductive polymer composites depends on the preparation technique. The filler particles should be well dispersed in the polymer matrix to prepare a proper composite material. Different preparation techniques are available to mix polymer and filler particles. In this study, graphite-filled EVA was obtained by combining solution and melt-mixing techniques. After dispersing graphite in EVA solution by magnetic stirring, the obtained composite material was deposited on a flat surface. Later on, it was extruded from the extruder head of FLM to ensure the proper dispersion of the graphite.

Scanning electron microscopy (SEM) images for all compositions of the developed composite surfaces were magnified to see the dispersion of graphite particles. SEM images depict the dispersion of graphite particles present in the EVA matrix with the variation of wt%. It can be seen that graphite particles are present in the developed composites but in a scattered way below 30 wt% of graphite content in EVA as shown in Fig. 6a–c. It means that there is no possible network formed between the graphite particles. As the graphite content is increased beyond this limit, the particles agglomerate and form conductive network due to the filler–filler interaction, which can be seen in Fig. 6d, e.

Further, X-ray diffraction (XRD) spectra of the pure EVA copolymer and graphite is recorded to show the presence and dispersion of filler particles in the polymer matrix as shown in Fig. 7. Graphite has a pronounced peak at $2\theta = 26.92°$ which is attributed to the diffraction of the crystalline phase of graphite, while the EVA shows diffraction peak at $2\theta = 21.94°$. Two peaks in the XRD spectra of developed composites show the presence of graphite and dispersion in the EVA matrix. The first peak is attributed to the EVA, while the second peak is generated due to the presence of graphite.

Chemical structural changes of the developed composite were depicted using Fourier transform infrared spectroscopy (FTIR) technique. Figure 8 shows the recorded FTIR spectra for EVA, graphite (Gr), and EVA/Gr composites. The spectrum of graphite does not show any noticeable peaks while EVA spectrum shows the various peaks at different regions. Generally, EVA spectra show the typical bands of VA at 1734, 1234, 1018, and 607 cm^{-1}, and ethylene at 2915, 2846, 1460, 1367, and 720 cm^{-1} [22–24]. The obtained peaks in EVA spectra are in good agreement with the literature values.

The peak (C=O) around 1736 cm^{-1} belongs to the carbonyl group and has great importance. It can be seen that the intensity of this peak decreases after the addition of graphite in EVA matrix. In addition, one fact can be noted that EVA/Gr composite spectrum have all the characteristic peaks for pure graphite and pure EVA. No new peaks are

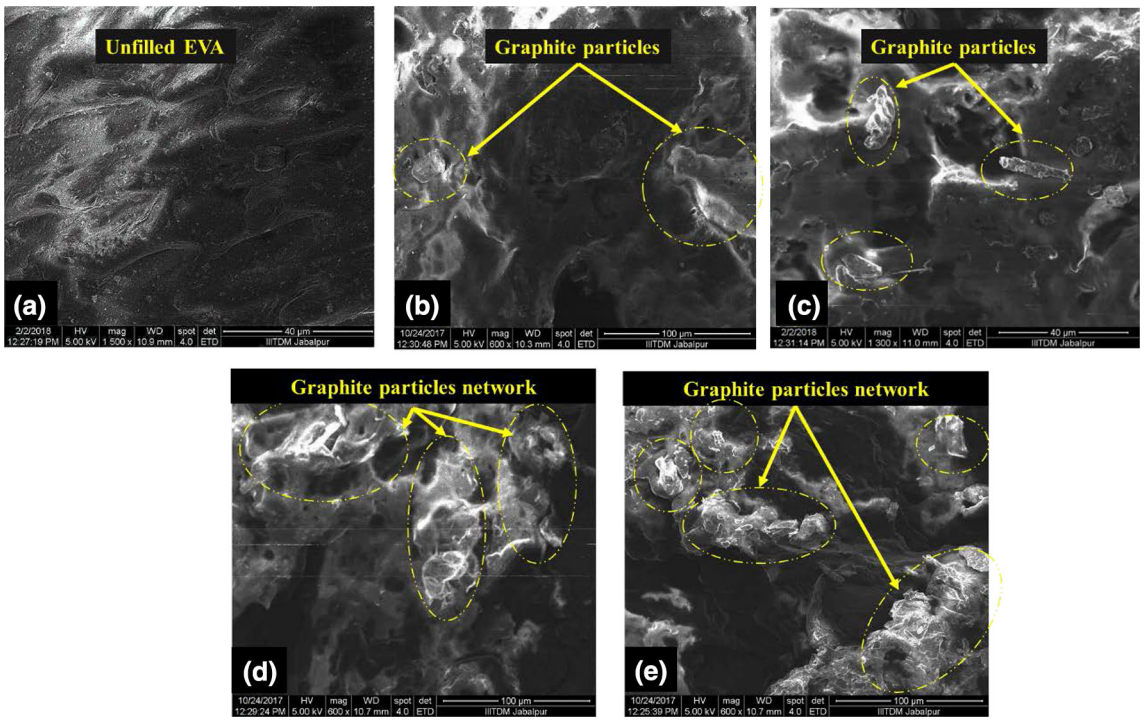

Fig. 6 SEM images of EVA/Gr (wt%/wt) **a** 100/0, **b** 80/20, **c** 70/30, **d** 60/40 and **e** 50/50

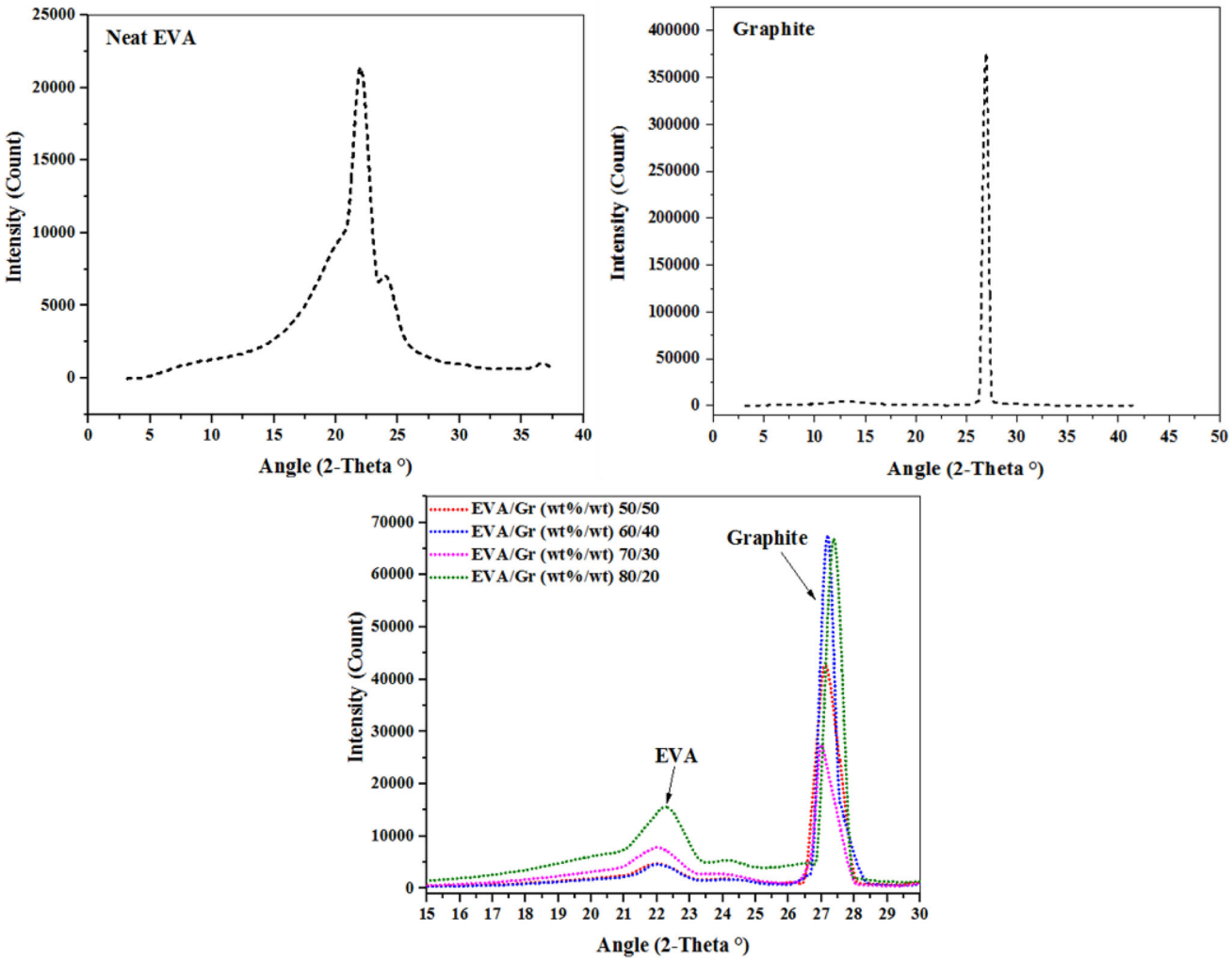

Fig. 7 XRD spectra of developed EVA/Gr composites

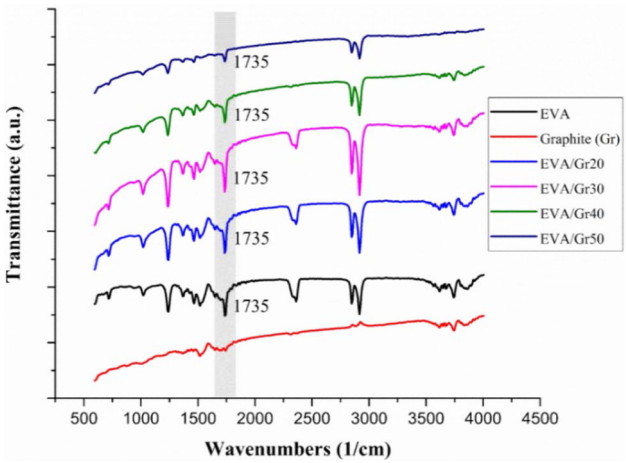

Fig. 8 FTIR spectra for the different combinations of EVA/Gr composites

observed which indicate the lack of interaction or reaction between EVA and graphite, which supports the obtained XRD results. In addition, it can be noticed that there is no observed shifting in characteristic peak which confirms the above statement.

After morphological analysis, rheological behavior of the developed composite has been observed. Melt flow rate (MFR) and swelling behavior of the developed composite have been measured to determine the proper road gap, layer thickness and the material deposition speed for different categories of developed EVA/Gr composite. As compared to EVA, the MFR of EVA/Gr composite decreases with the increment in the filler contents. It shows that deposition speed is varied for each category of the composite, the effect of MFR results can be seen in Fig. 9 where the deposition speed used in the study has been decreased as the filler contents increased in the EVA matrix. A similar trend has been observed in the swelling behavior of the developed composite. Swelling is decreased as the filler contents increased. It suggests that the value of deposition speed and road gap will be reduced,

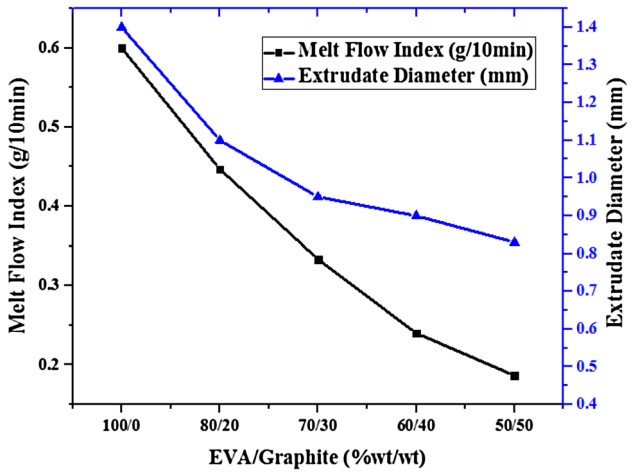

Fig. 9 Recorded extruded diameter and MFI values of EVA and EVA/Gr composites

as the part printing will be done with highly Gr-filled composites.

Usually, the high amount of filler loading in composites hinders the melt flow rate because it increases the filler–filler interaction. The evidence is obtained in captured SEM images of the developed composites having 20, 30, 40 and 50% amount of graphite loading. On the other hand, swelling of the polymers depends on the elastic recovery of the polymer melt. Filler loading in the polymer matrix affects the elastic recovery, and it decreases with increasing amount of filler loading due to filler particle interaction in the reported literature. The evidence can be seen in the obtained results, where the diameter of extruded EVA/Gr composites decreases gradually with increasing of filler loading (wt%).

3.2 Flexible electrically conductive parts through developed FLM

Developed FLM is an extrusion-based process that involves the partial melting of pellets in the form of roads to create three-dimensional parts by depositing material in a layer-by-layer fashion. After each layer is deposited, FLM extruder head goes up by a one layer thickness, a new layer of material is deposited on the top of previously deposited layer, and the process is repeated until the whole part is fabricated. During the FLM processing, the graphite particles were dispersed finely in the EVA matrix due to rotating screw inside the barrel. The evidence can be seen in SEM images. Figure 10 shows the specimens fabricated using EVA and EVA/Gr composites. These fabricated specimens were used for electrical and mechanical testing. The top and side surfaces of the specimens were examined by capturing microscopic images. It can be seen that multiple roads or layers are uniformly placed as per the given road width. The interface bonding between adjacent layers or roads was good enough to merge them.

The flexibility of the printed specimens is shown in Fig. 11. The fabricated tensile specimen is manually bent in different directions to demonstrate the flexibility aspects of the investigated composite specimen.

3.3 Sample characterization

The electrical conductivities of EVA and EVA/Gr combinations have been determined using four-probe method. Figure 12 shows the obtained results for electrical conductivities.

It can be seen that electrical conductivity of graphite-filled EVA is increased as compared to pure EVA material. There is little increase in the electrical conductivity of FLM-processed EVA/Gr composites with the graphite contents of 20 and 30 wt%. However, a sudden jump in the electrical conductivity has been observed when Gr content is further increased up to 40 and 50 wt%. It implies that graphite particles make the connected networks at high wt% due to their better dispersion in EVA matrix during the mixing process. The evidence can be seen in the SEM images. The minimum and maximum electrical conductivities are 4.2×10^{-7} and 2.3×10^{-4} S cm^{-1} for EVA and EVA/GR50 composite, respectively, which is 539 times for EVA/Gr50 composites as compared to EVA.

To predict the electrical conductivity of any polymer composites, classical percolation theory is widely used. According to this theory, the polymer composite can achieve electrical conductivity when the volume/weight fraction of filler material is above the specified value. This particular value of volume/weight fraction is known as percolation threshold. The schematic representation of electrical percolation threshold for EVA/Gr composites is shown in Fig. 13. It can be anticipated that at low graphite concentration, the electrical conductivity of the EVA/Gr composites is comparable to the neat EVA material. The start of electrical conductivity can be seen when the graphite particles come closer to one another and form the connecting networks at percolated threshold point. The reported literature shows percolation threshold value for graphite around 30 wt% (16 vol%) [25]. The obtained results of the current study are in good agreement with the reported results.

It can be observed that electrical conductivity of developed EVA/graphite composite is approximately close to the electrical conductivity of neat EVA below 30 wt% fraction. Above 30 wt%, the electrical conductivity of developed EVA/graphite composites starts shifting toward the higher side due to the formation of conductive networks of graphite particles. This is the reason for obtaining high

Fig. 10 Fabricated specimens using EVA and EVA/Gr40 composite, a microscopic image showing the bonding between roads

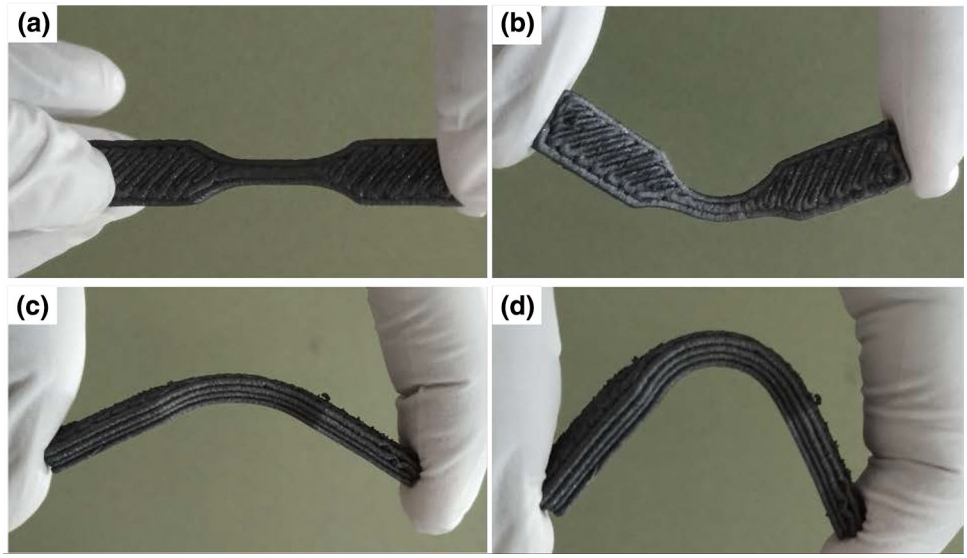

Fig. 11 **a** Fabricated specimen and **b–d** demonstrating flexibility in the fabricated specimen

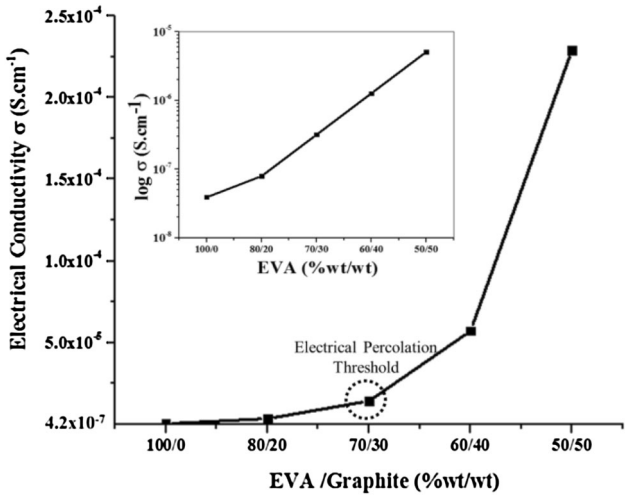

Fig. 12 Electrical conductivity of FLM-processed Gr-filled EVA composites. Inset: log plot of electrical conductivity for Gr-filled EVA composites

electrical conductivity value of developed composites at 50 wt% loading.

On the one hand, the addition of graphite in EVA matrix improves the electrical properties by maintaining proper flexibility (refer Fig. 11). However, on the other hand, the addition of graphite content in EVA matrix adversely affects the tensile properties of samples. The dependencies of tensile strength and elongation at the break on the wt% of filler content are shown in Fig. 14a. The results clearly show the significant drop in tensile strength and elongation at break of the specimens after addition of graphite content in EVA matrix. Similar results have been found in the literature for other composite materials [5, 26, 27]. The obtained results can be attributed to the lack of interaction between the graphite and EVA materials. As discussed, XRD and FTIR result also confirm this lack of interaction. Due to this, voids were created between graphite particles and EVA matrix in the developed composites, which resulted in the decrease in tensile properties as shown in Fig. 14b–d. Moreover, the variation in delay time (time

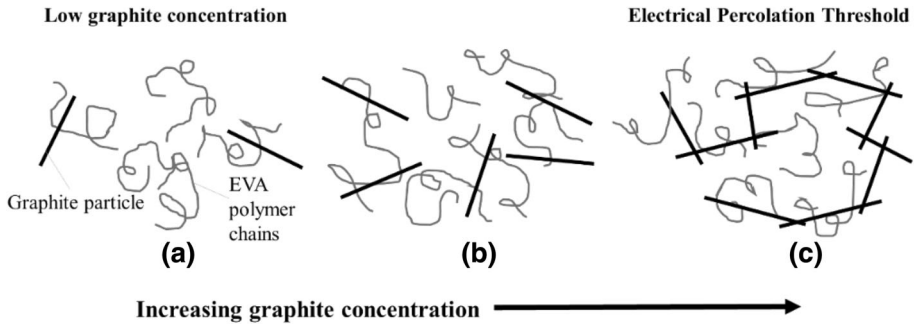

Fig. 13 Schematic representation electrical percolation threshold for EVA/Gr composites

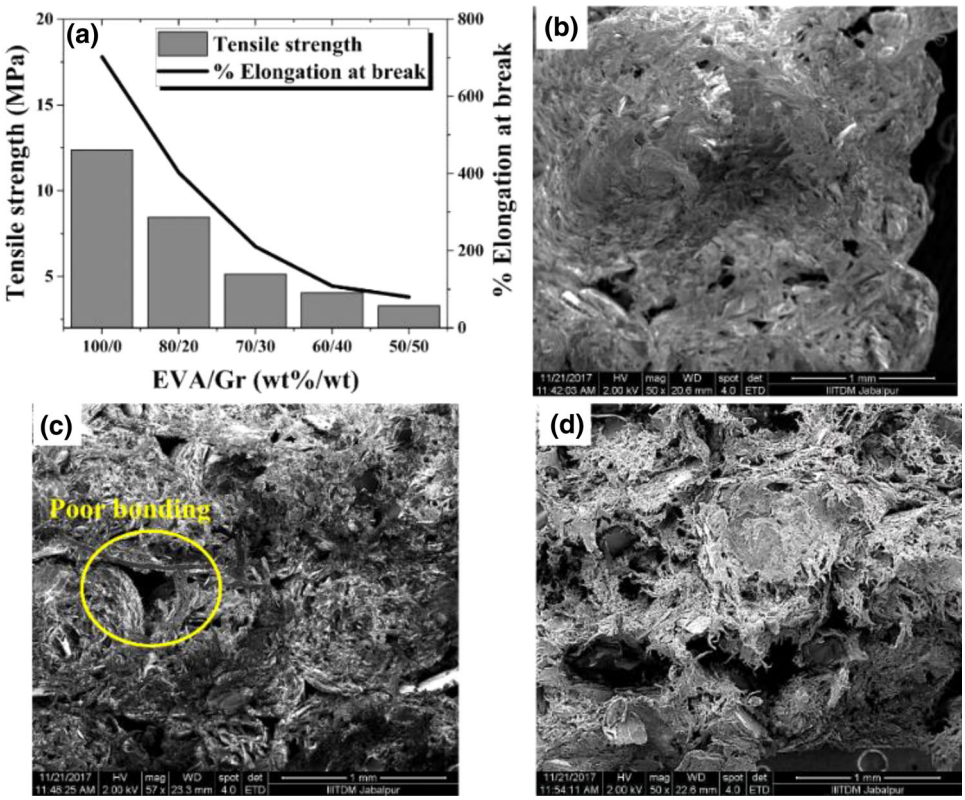

Fig. 14 **a** Variation of tensile properties with the increase of graphite content and SEM images of the fracture surfaces of EVA/Gr composites **b** 70/30, **c** 60/40 and **d** 50/50

difference for material deposition between any two adjacent points on successive roads in a layer) during fabrication of specimens through FLM can be another reason behind degrading tensile properties. The delay in material deposition occurred due to the printing of specimens for each compositions at different deposition speeds. When the delay is more, polymer diffusion across the roads will be less due to large temperature difference, as a result, weak road bonding will be observed and vice versa [28]. Due to this, most degradation in the tensile properties was observed with the specimens printed with minimum deposition speed i.e., EVA/Gr (50/50).

After analyzing the tensile properties, compression testing has been performed on the fabricated specimens. The testing is performed up to 40% deformation of the original specimen height. The obtained results are shown in Fig. 15. In comparison to EVA specimen, an increase of 172.5% was reported in the fabricated EVA/graphite (50/50) composite specimens. The obtained results can be attributed to the presence of graphite particles in the EVA matrix. Graphite is a stronger candidate than EVA which bears the compressive load conveyed by the EVA matrix and increases the load-bearing ability of the composite specimens. Tested specimens showed the spring back effect after the load removal. This behavior shows the flexible nature of the fabricated specimens.

Further, the effect of graphite content on the hardness of EVA matrix has been analyzed. The hardness of developed EVA/Gr composites was measured using the digital durometer (shore D) and compared with the hardness of EVA material. Figure 16 shows the hardness results obtained for EVA and EVA/Gr composites. Based on the

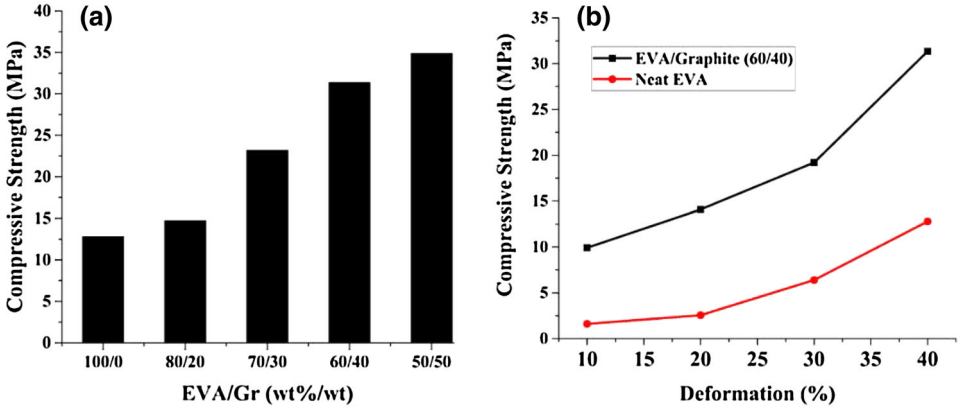

Fig. 15 **a** The variation of compressive strength with the increase of graphite content, **b** compressive strength vs. deformation (%) for neat EVA and EVA/graphite (60/40)

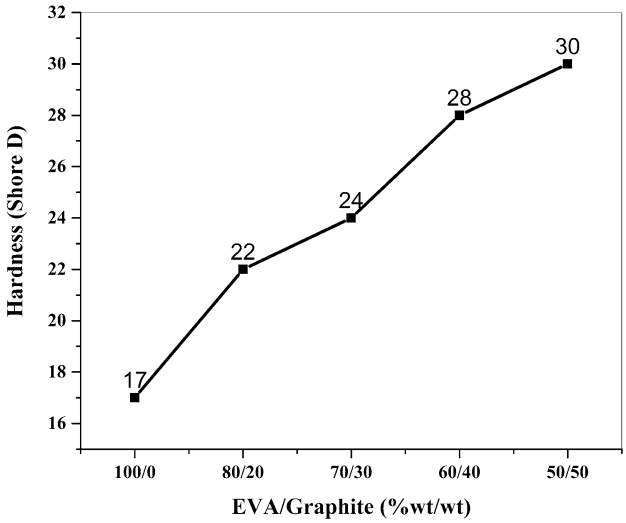

Fig. 16 Obtained hardness results

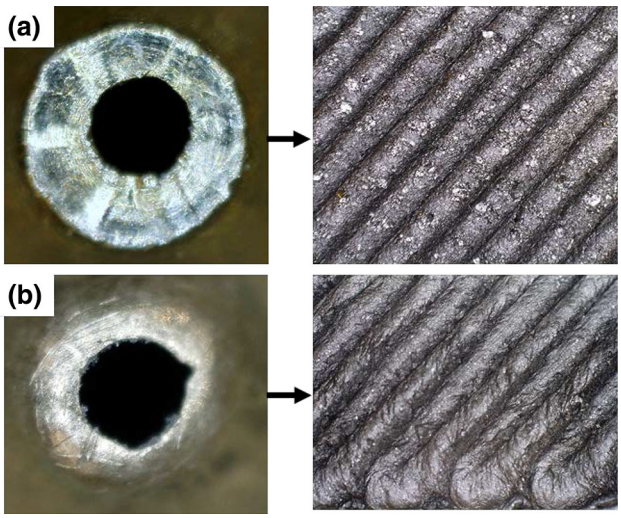

Fig. 17 Microscopic images showing the nozzle-opening surface after the printing with EVA/Gr composites and corresponding printed surface **a** 80/20 and **b** 60/40

results, the addition of graphite increases the hardness of EVA. It is self-explanatory that hardness of graphite is much higher than the hardness of EVA. In addition, it has been reported in the literature that improvement in the hardness does not depend only on the hardness of filler particles, but the good dispersion of fillers can also influence the hardness. Therefore, the obtained result can be attributed to the proper dispersion and formation of interconnecting network structures of graphite particles within EVA matrix. The hardness value for pure EVA is 17 (shore D), and it is increased up to 30 (shore D) with the addition of 50 wt% of graphite.

3.4 Nozzle wear

The continuous extrusion and deposition of graphite-filled EVA may lead to wear in nozzle opening. Therefore, the nozzle diameter was examined before and after the printing of specimens to see the effect of filler particles on nozzle diameter and geometry. Microscopic images were taken after proper cleaning of the nozzle. Figure 17 shows the nozzle surface after printing with EVA/Gr composites of 80/20 and 60/40. Upon continued deposition, the copper nozzle quality was abraded on the front surface as well as on the inside of the nozzle. It occurs because the nozzle touches the fabricated object during the deposition. Obtained results show that abrasion of the nozzle is not affected by the electrical and mechanical properties, only small loss in printing resolution is observed. This issue can be overcome in future work in which nozzle made with hard materials may be used for printing composite materials.

4 Conclusions

In this work, an approach to fabricate flexible electrically conductive parts using EVA and graphite was presented. A customized extrusion-based FLM system was developed to

carry out the current study. The electrical conductivity, morphology, printability, rheological and mechanical properties were evaluated to investigate future possibilities of developed EVA/Gr composites. The electrical conductivity of FLM-processed EVA/Gr composites filled with 50 wt% graphite achieves 2.3×10^{-4} S cm^{-1} which is 539 times of the electrical conductivity of neat EVA. The obtained improvement in electrical conductivity implies the formation of conductive networks at higher wt% of graphite. The tensile properties of the EVA showed the strong dependence on the addition of graphite particles. Tensile strength and elongation at break were decreased by 73 and 88.60%, respectively, as compared to the properties of unfilled EVA. The addition of graphite created the voids in the EVA matrix and worked as defects, which reduces the tensile properties of the specimens prepared by EVA/Gr composites. Moreover, the variation in delay time during fabrication of specimens through FLM was another reason behind degrading tensile properties. However, the compressive properties and hardness of the developed composite showed the opposite trend and increased with the addition of graphite particles. This trend is attributed to the strongness of graphite particles as compared to EVA, due to which, the composite specimens showed the increase in load-bearing capacity. The current study is an initial step towards the development of flexible composites, which helps in finding suitable wt% of graphite to make EVA material conductive with a desired flexibility. Most importantly, the developed composite remain printable through developed FLM process even after adding graphite up to 50 wt%. Overall, the study demonstrated that FLM is a viable process and can be used to fabricate flexible electrically conductive parts.

Acknowledgements Authors gratefully acknowledge the financial support received from SERB-DST for carrying the present research work.

References

1. Qin Y, Howlader MMR, Deen MJ et al (2014) Polymer integration for packaging of implantable sensors. Sens Actuators B Chem 202:758–778. https://doi.org/10.1016/j.snb.2014.05.063
2. Li Y, Liu Z, Wang T, Shang S (2016) High-piezoresistive sensitivity of silicone matrix composites with low metal filler content. Mater Lett 171:252–254. https://doi.org/10.1016/j.matlet.2016.02.093
3. Taherian R (2016) Experimental and analytical model for the electrical conductivity of polymer-based nanocomposites. Compos Sci Technol 123:17–31. https://doi.org/10.1016/j.compscitech.2015.11.029
4. Alam A, Meng Q, Shi G et al (2016) Electrically conductive, mechanically robust, pH-sensitive graphene/polymer composite hydrogels. Compos Sci Technol 127:119–126. https://doi.org/10.1016/j.compscitech.2016.02.024
5. Zhao W, Nugay II, Yalcin B, Cakmak M (2016) Flexible, stretchable, transparent and electrically conductive polymer films via a hybrid electrospinning and solution casting process: in-plane anisotropic conductivity for electro-optical applications. Displays 45:48–57
6. Goodridge RD, Shofner ML, Hague RJM et al (2011) Processing of a Polyamide-12/carbon nanofibre composite by laser sintering. Polym Test 30:94–100. https://doi.org/10.1016/j.polymertesting.2010.10.011
7. Sefadi JS, Luyt AS (2012) Morphology and properties of EVA/empty fruit bunch composites. J Thermoplast Compos Mater 25:895–914. https://doi.org/10.1177/0892705711421806
8. Kumar N, Shaikh S, Jain PK, Tandon P (2015) Effect of fractal curve based toolpath on part strength in fused deposition modelling. Int J Rapid Manuf 5:186–198. https://doi.org/10.1504/IJRAPIDM.2015.073576
9. Shaikh S, Kumar N, Jain PK, Tandon P (2016) Hilbert curve based Toolpath for FDM process. In: CAD/CAM, robot factories future. Springer, New Delhi, pp 751–759
10. Taufik M, Jain PK (2016) A study of build edge profile for prediction of surface roughness in fused deposition modeling. J Manuf Sci Eng 138:1–11. https://doi.org/10.1115/1.4032193
11. Taufik M, Jain PK (2013) Role of build orientation in layered manufacturing: a review. Int J Manuf Technol Manag 27:47–73. https://doi.org/10.1504/IJMTM.2013.058637
12. Masood SH, Song WQ (2005) Thermal characteristics of a new metal/polymer material for FDM rapid prototyping process. Assem Autom 25:309–315. https://doi.org/10.1108/01445150510626451
13. Torrado Perez AR, Roberson DA, Wicker RB (2014) Fracture surface analysis of 3D-printed tensile specimens of novel ABS-based materials. J Fail Anal Prev 14:343–353. https://doi.org/10.1007/s11668-014-9803-9
14. Nikzad M, Masood SH, Sbarski I (2011) Thermo-mechanical properties of a highly filled polymeric composites for fused deposition modeling. Mater Des 32:3448–3456. https://doi.org/10.1016/j.matdes.2011.01.056
15. Boparai KS, Singh R, Singh H (2016) Experimental investigations for development of Nylon6-Al-Al_2O_3 alternative FDM filament. Rapid Prototyp J 22:217–224. https://doi.org/10.1108/RPJ-04-2014-0052
16. Wei X, Li D, Jiang W et al (2015) 3D printable graphene composite. Sci Rep 5:11181. https://doi.org/10.1038/srep11181
17. Rymansaib Z, Iravani P, Emslie E et al (2016) All-polystyrene 3D-printed electrochemical device with embedded carbon nanofiber-graphite-polystyrene composite conductor. Electroanalysis 28:1517–1523. https://doi.org/10.1002/elan.201600017
18. Gnanasekaran K, Heijmans T, van Bennekom S et al (2017) 3D printing of CNT- and graphene-based conductive polymer nanocomposites by fused deposition modeling. Appl Mater Today 9:21–28. https://doi.org/10.1016/j.apmt.2017.04.003
19. Leigh SJ, Bradley RJ, Purssell CP et al (2012) A simple, low-cost conductive composite material for 3D printing of electronic sensors. PLoS One 7:1–6. https://doi.org/10.1371/journal.pone.0049365
20. Kwok SW, Goh KHH, Tan ZD et al (2017) Electrically conductive filament for 3D-printed circuits and sensors. Appl Mater Today 9:167–175. https://doi.org/10.1016/j.apmt.2017.07.001
21. Kumar N, Jain PK, Tandon P, Pandey PM (2018) Extrusion-based additive manufacturing process for producing flexible parts. J Braz Soc Mech Sci Eng 40:143. https://doi.org/10.1007/s40430-018-1068-x
22. Landete-Ruiz MD, Martín-Martínez JM (2005) Surface modification of EVA copolymer by UV treatment. Int J Adhes Adhes 25:139–145. https://doi.org/10.1016/j.ijadhadh.2004.06.001

23. Guo C, Zhou L, Lv J (2013) Effects of expandable graphite and modified ammonium polyphosphate on the flame-retardant and mechanical properties of wood flour-polypropylene composites. Polym Polym Compos 21:449–456. https://doi.org/10.1002/app
24. Bidsorkhi HC, Adelnia H, Heidar Pour R, Soheilmoghaddam M (2015) Preparation and characterization of ethylene-vinyl acetate/halloysite nanotube nanocomposites. J Mater Sci 50:3237–3245. https://doi.org/10.1007/s10853-015-8891-6
25. Tavman I, Turgut A, Horny N, Chirtoc M (2013) Polymer matrix composites reinforced with expanded and unexpanded graphite Particles for electronic packaging applications. In: 2013 IEEE 19th int symp des technol electron packag SIITME 2013—Conf Proc, pp 43–47. https://doi.org/10.1109/siitme.2013.6743642
26. Therriault Daniel, Hughes Vincent, Ilyass Tabiai KC (2016) 3D printable conductive nanocomposites of PLA and MWCNT. Mater Matters 11:61–65. https://doi.org/10.13140/RG.2.2.17004.16007
27. Hu W, Chen S, Yang Z et al (2011) Flexible electrically conductive nanocomposite membrane based on bacterial cellulose and polyaniline. J Phys Chem B 115:8453–8457
28. Jain PK, Pandey PM, Rao PVM (2009) Effect of delay time on part strength in selective laser sintering. Int J Adv Manuf Technol 43:117–126. https://doi.org/10.1007/s00170-008-1682-3